

## Article

# A Correction Method for the Motion Measurement of the Ship-Borne Mechanical Platform Based on Multi-Sensor Fusion

Rongqiang Zhao and Xiong Hu \*

Logistics Engineering College, Shanghai Maritime University, Shanghai 201306, China

\* Correspondence: huxiong@shmtu.edu.cn

**Abstract:** In order to perform multi-degree-of-freedom motion measurements of marine machinery, such as ship-borne mechanical platforms, in an absolute environment without a reference, absolute measurement methods using acceleration sensors and tilt gyroscopes are typically employed. However, the influence of wave forces on ship-borne mechanical platforms can cause coupling between different degrees of freedom, resulting in significant measurement disturbances that make efficient computation and real-time analysis challenging. To address these challenges, a correction method for the motion measurement of the ship-borne mechanical platform based on multi-sensor fusion is proposed by analyzing the influence of the inclination angle of the ship-borne mechanical platform on the sensor measurement based on the working principles of the acceleration sensor and angle sensor. In this article, we first analyzed the influence of the inclination angle on the integral effect in the heave direction. Then, we proposed a configuration using four groups of acceleration sensors to correct the integral effect. Finally, the optimal inclination angle is determined through Kalman filtering based on the measured values of the angle sensors and estimated values from the acceleration sensor sets. Experiments have proved that the average error of the corrected heave displacement signal is 25.34 mm, which is better than the integral displacement signal of a single acceleration sensor. At the same time, we use the acceleration sensor to calculate the roll angle and pitch angle of the ship-borne mechanical platform and combine it with the angle sensor signal to perform Kalman filtering. This filters out the errors caused by the shaking and instability of the mechanical platform and can more accurately estimate the true inclination of the platform. Therefore, this method can enhance the precision and accuracy of ship-borne mechanical platform motion signal acquisition, providing more valuable experimental data for research in marine engineering and related fields.

**Keywords:** acceleration sensor; angle sensor; multi-sensor fusion; Kalman filter; signal acquisition



**Citation:** Zhao, R.; Hu, X. A Correction Method for the Motion Measurement of the Ship-Borne Mechanical Platform Based on Multi-Sensor Fusion. *Machines* **2023**, *11*, 847. <https://doi.org/10.3390/machines11080847>

Academic Editor: Zheng Chen

Received: 25 July 2023

Revised: 19 August 2023

Accepted: 20 August 2023

Published: 21 August 2023



**Copyright:** © 2023 by the authors. Licensee MDPI, Basel, Switzerland. This article is an open access article distributed under the terms and conditions of the Creative Commons Attribution (CC BY) license (<https://creativecommons.org/licenses/by/4.0/>).

## 1. Introduction

Due to the motion experienced by ship-borne mechanical platforms on the sea, it is essential to consider the three degrees of freedom: heave, roll, and pitch. Typically, the motion signal in the heave direction is acquired through double integration of data from an acceleration sensor. However, ship-borne mechanical platforms also experience movements in roll and pitch directions, which can cause the acceleration sensor to deviate from the ideal horizontal plane. These inclination angles cause additional horizontal forces to be exerted on the piezoelectric element of the acceleration sensor, leading to errors in the displacement measurement obtained through integration. As a result, it becomes difficult to accurately calculate the behavior of the ship-borne mechanical platform.

The key concerns in estimating the behavior of ship-borne mechanical platforms are mainly about improving the accuracy and real-time performance of the sensor system, particularly under the influence of low-frequency motion caused by sea waves. Challenges arise as each type of sensor has its limitations and cannot solely obtain accurate multi-dimensional behavior data. Aggressively increasing the number of sensors is not a wise solution, as it brings a massive computational burden. To achieve a precise estimation of

ship-borne mechanical platform behavior while eliminating information redundancy, an efficient multiple-sensor fusion method with multilevel information processing abilities is required.

To address the shortcomings of a single sensor in accurately estimating real-time and comprehensive multi-degree-of-freedom information, scholars have conducted extensive research on multi-sensor fusion techniques. Luo R.C. proposed the sensor data fusion system in 1988 [1]. Durrant-Whyte H.F. developed a fully decentralized architecture for data fusion problems in 1990 [2]. Wen W. in 1992 described an algorithm for implementing multi-sensor systems considering constraints in a model-based environment [3]. Harris C.J. formally introduced the process of data fusion and sensor integration and various implementation architectures in 1998, considering data fusion as a key element of the overall system integration [4]. Llinas J. provided a tutorial on data fusion in 1998, presenting data fusion applications, process models, and the identification of suitable techniques [5]. Chen S. designed a multi-sensor data fusion system in 2003 [6]. Herpel T. conducted a study in 2008 on the impact of combining sensor data at different abstraction levels on the performance of multi-sensor systems [7]. In the same year, Manjunatha P. proposed a multi-sensor data fusion algorithm in WSN [8]. Dong J. presented an overview of recent advances in multi-sensor fusion [9]. Wolter P.T. used partial least squares regression to integrate different combinations of satellite sensor data in 2010 [10]. Medjahed H. proposed an automatic in-home healthcare monitoring system with several sensors in 2011 [11]. Banerjee T.P. proposed a method for fault signal classification based on sensor data fusion in 2012 [12]. Frikha A. proposed a method to determine the weights of a sensor reading set [13]. Azimirad E. presented a comprehensive review of data fusion architecture in 2015 [14]. In the same years, G. Fortino proposed a system based on a multi-sensor data fusion schema [15]. S. Rawat used a neural network to solve an inherent problem of multi-sensor data fusion in 2016 [16]. Duro J.A. proposed a novel multi-sensor data fusion framework in 2016 [17]. Maimaitijiang M. used thermal data fusion to estimate parameters in 2017 [18]. Jing L. proposed an adaptive multi-sensor data fusion method for fault diagnosis in 2017 [19]. Kumar P. proposed a multi-sensor fusion framework in 2017 [20]. Bouain M. proposed a multi-sensor data fusion (MSDF) in 2018 [21]. Xiao F. proposed a method for multi-sensor data fusion in 2018 [22]. Zhang W. proposed a model based on multi-sensor data fusion in 2019 [23]. De Farias C.M. proposed a technique that attributes an interval to an abstract sensor in 2019 [24]. Xiao F. proposed a method for multi-sensor data in 2019 and then proposed a hybrid MSDF method in 2020 [25,26]. Muzammal M. proposed a data fusion-enabled ensemble approach in 2020 [27]. Li N. proposed a method based on a multi-sensor data fusion model in 2021 [28]. Kashinath S.A. reviewed methods used for real-time and multi-sensor studies in 2021 [29]. Fei S. proposed a method based on multi-sensor data that can improve prediction accuracy in 2023 [30]. Han C. proposed an absolute displacement measurement method in 2023 [31]. R.G. Wright integrated the multi-sensor fusion method into autonomous ships in 2019 [32]. R. Ma proposed a target fusion algorithm based on multisensory information in 2020 [33]. U. Ali proposed a solution based on a board sensor in 2021 [34]. E. Higgins evaluated data fusion algorithms in 2022 [35]. However, in the field of three-degree-of-freedom motion measurement of ship-borne mechanical platforms, the method of multi-sensor fusion has been seldom used. There are still many technical problems in the application of ship-borne mechanical platform motion measurements. Especially, the inherent interference between the effects of different degree-of-freedom ship movements on sensor outputs causes challenges to traditional sensor-fusion methods.

In this paper, we propose a ship-borne mechanical platform motion measurement correction method based on multi-sensor fusion to improve the accuracy of the ship-borne mechanical platform motion signal computed by the double integration of the single-degree-of-freedom acceleration sensor. The proposed sensor configuration includes a set of angle sensors and four sets of acceleration sensors, which eliminates the influence of the inclination angle on the integral displacement signal in the heave direction. We utilize

the Kalman filter to estimate the optimal inclination angle and heave displacement. In the proposed Kalman filtering-based algorithm, we use the calculated angle signal as the estimation value and the angle signal collected by the angle sensor as the observation value to iteratively optimize the inclination angles. In order to prove the effectiveness of the method, we verified the proposed algorithm on the laboratory platform by simulating the motion of the ship-borne mechanical platform and computing the multi-sensor fusion heave displacement estimation. Finally, we compared the estimated data with the standard motion signal obtained by a laser sensor. It is verified that the algorithm based on the data fusion of acceleration sensors and tilt angle sensors can restore the actual motion characteristics of the ship-borne mechanical platform more precisely than methods using only one type of motion sensor.

The main contributions of this paper are summarized as follows:

1. A method for measuring and correcting the heave direction of ship-borne mechanical platform motion based on multi-acceleration-sensor fusion is proposed. The heave displacement signal of the platform under an unknown tilt angle is calculated by the outputs of four sets of acceleration sensors with improved accuracy.
2. A method for measuring the change in inclination angle of ship-borne mechanical platform motion based on the Kalman filtering technique using sensor fusion of an acceleration sensor and an angle sensor is proposed. The calculated tilt angle of the platform in roll and pitch directions calculated by four sets of acceleration sensors is used as the estimation value, and the inclination angle signal measured by the angle sensor is used as the observation value. Innovation-based adaptive Kalman filtering is used to obtain the inclination angle and the heave displacement of the platform with higher accuracy.

The subsequent sections of this manuscript are organized as follows: Section 2 presents the effect of tilt angle on the integrated displacement signal in the heave direction. Section 3 details the correction principle and the proposed correction method for ship-borne mechanical platform motion measurement based on multi-sensor fusion. Section 4 designs experiments to verify the effectiveness of the ship-borne mechanical platform motion measurement correction method based on multi-sensor fusion. Section 5 presents the conclusion and provides suggestions for future work.

## 2. Preliminary Work

There are two main types of acceleration sensors at present: piezoelectric sensors and capacitive sensors. Both sensors output acceleration-related signals, but with different working mechanisms.

Capacitive acceleration sensors use changes in capacitance to measure acceleration. It usually consists of two parallel metal plates with a central mass. When the sensor is subjected to acceleration, the mass will be displaced relative to the metal plate, thereby changing the capacitance value between the metal plates. By measuring the change in the capacitance value, the acceleration experienced by the sensor can be calculated.

Piezoelectric acceleration sensors use the piezoelectric effect for measurement. It usually consists of one or more piezoelectric crystals, a vibrating proof mass, and signal processing circuitry. When the sensor is subjected to acceleration, the vibrating proof mass compresses or stretches the piezoelectric crystal, which creates an electrical charge and generates a voltage signal. The signal processing circuit will amplify, filter, and digitize the voltage signal to finally obtain the measured value of acceleration.

However, in ship-borne mechanical platform motion measurement, capacitive sensors have many disadvantages:

1. Capacitance is seriously interfered with by the marine environment, such as temperature, humidity, and other factors. Generally, it needs to be shielded and filtered; otherwise, it will affect the measurement accuracy.
2. Capacitive sensors need to be installed on the hull, which is easily subjected to vibration and shock from the hull.

3. In marine environments, capacitive sensors are susceptible to seawater corrosion and water pressure, requiring special protection methods.

Piezoelectric sensors are known to be sensitive to temperature drifts and humidity. The sensitivity of the sensor to these environmental factors can lead to measurement errors and reduced accuracy. To mitigate these effects, several techniques have been proposed, such as temperature compensation and humidity shielding. Temperature compensation involves designing the sensor to be insensitive to temperature changes by using materials with a low coefficient of thermal expansion. Humidity shielding involves coating the sensor with a material that is impermeable to water vapor, such as polytetrafluoroethylene (PTFE), to prevent moisture from affecting the sensor's performance. These techniques can help improve the accuracy and reliability of piezoelectric sensors in various applications.

Therefore, piezoelectric sensors are usually more suitable for use in ship-borne mechanical platform motion measurements. Piezoelectric sensors are not affected by harsh environments such as high temperature and high pressure and have better anti-interference abilities, which provide more accurate measurement results. We will discuss the acceleration sensor based on piezoelectric effects in the rest of the article.

During the process of measuring acceleration with a piezoelectric sensor, the output results can be directly affected by vertical and horizontal movements, such as pitching and rolling. These movements can alter the orientation of the sensor and therefore affect the accuracy of measurements. Additionally, any tilting movements can also impact the sensor's signal, in addition to any coupling effects on the overall system. Mainly because any movement or tilting of the acceleration sensor can affect the orientation of the mass within the device and therefore alter the output signal. For example, if the acceleration sensor is tilted to one side, the gravitational force acting on the mass will be shifted, leading to inaccurate measurements. Similarly, if the acceleration sensor is subjected to any pitching or rolling movements, the direction of gravitational force will change and affect the measurements accordingly.

To compensate for these effects, it is important to properly calibrate the acceleration sensor and account for any potential sources of error. This can include adjusting for any tilting or coupling effects. The influence of the inclination angle on the integrated displacement signal in the heave direction is shown in Figure 1.

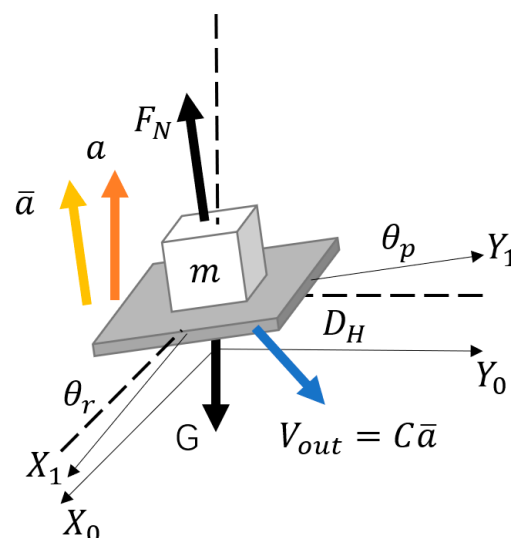


**Figure 1.** Schematic diagram of the influence of inclination angle on the integrated displacement signal in the heave direction.

When the ship-borne mechanical platform is in its horizontal position, the relationship between the heave acceleration and the support force  $F_N$ , of the ship-borne mechanical platform to the acceleration sensor is given by

$$F_N - G = ma, \quad (1)$$

where  $m$  and  $G$  are the mass and the gravity force of the proof mass, respectively. As the output voltage of the piezoelectric sensor  $V_{out}$  is approximately linear to the applied stress, we obtain that

$$V_{out} = \frac{(F_N - G)}{K}, \quad (2)$$

where  $K$  is the linearized piezoelectric coefficient. The sensitivity  $C$  of the acceleration sensor could be expressed as

$$C = \frac{V_{out}}{a} = \frac{K}{m}. \quad (3)$$

However, in real-world applications, pitch angle  $\theta_p$  and roll angle  $\theta_r$  tilt the ideal coordinates, and the data should be accordingly adjusted in real-time. The transformation matrix from the earth coordinate system to the accelerator platform coordinate system is obtained as follows:

$$\begin{aligned} R_{xy}^t &= \begin{pmatrix} 1 & 0 & 0 \\ 0 & \cos\theta_p^t & -\sin\theta_p^t \\ 0 & \sin\theta_p^t & \cos\theta_p^t \end{pmatrix} \begin{pmatrix} \cos\theta_r^t & 0 & \sin\theta_r^t \\ 0 & 1 & 0 \\ -\sin\theta_r^t & 0 & \cos\theta_r^t \end{pmatrix} \begin{pmatrix} 1 & 0 & 0 \\ 0 & 1 & 0 \\ 0 & 0 & 1 \end{pmatrix} \\ &= \begin{pmatrix} \cos\theta_r^t & \sin\theta_p^t \sin\theta_r^t & \cos\theta_p^t \sin\theta_r^t \\ 0 & \cos\theta_p^t & -\sin\theta_p^t \\ -\sin\theta_r^t & \sin\theta_p^t \cos\theta_r^t & \cos\theta_p^t \cos\theta_r^t \end{pmatrix}. \end{aligned} \quad (4)$$

Since the acceleration sensor only measures normal acceleration in the  $O-X_1Y_1$  plane, the detected acceleration  $\bar{a}$  could be calculated by

$$\bar{a} = \frac{F_N - G \cos\theta_r \cos\theta_p}{m}. \quad (5)$$

Therefore, the output voltage of the piezoelectric sensor is

$$V_{out} = \frac{F_N - G \cos\theta_r \cos\theta_p}{K} = \frac{\bar{a} + \frac{G}{m}(1 - \cos\theta_r \cos\theta_p)}{C}. \quad (6)$$

The actual acceleration  $a$  of the sensor can be obtained by

$$a = \frac{\bar{a}}{\cos\theta_r \cos\theta_p} = \tilde{C}(\theta_r, \theta_p) V_{out} + \tilde{D}(\theta_r, \theta_p), \quad (7)$$

where  $\tilde{C}(\theta_r, \theta_p)$  and  $\tilde{D}(\theta_r, \theta_p)$  are the slope correction factor and intercept correction factor of the acceleration sensor, respectively, as follows:

$$\tilde{C}(\theta_r, \theta_p) = \frac{C}{\cos\theta_r \cos\theta_p} \quad (8)$$

and

$$\tilde{D}(\theta_r, \theta_p) = g \left( 1 - \frac{1}{\cos\theta_r \cos\theta_p} \right), \quad (9)$$

where  $g$  is the acceleration of gravity.

Now we assume that the accelerator has a displacement of  $dH$  in the heave direction. In other words, the movement of the sensor  $T_G$  can be denoted as:

$$dT_G = \begin{pmatrix} 0 \\ 0 \\ dH \end{pmatrix}. \quad (10)$$

During this small time period,  $\theta_p$  and  $\theta_r$  can be regarded as constant. Therefore, the displacement of the acceleration sensor  $T_L$  under the ship-borne mechanical platform coordinate system is computed as follows:

$$\begin{aligned} dT_L &= R_{xy}^t dT_G = \begin{pmatrix} \cos\theta_r^t & \sin\theta_p^t \sin\theta_r^t & \cos\theta_p^t \sin\theta_r^t \\ 0 & \cos\theta_p^t & -\sin\theta_p^t \\ -\sin\theta_r^t & \sin\theta_p^t \cos\theta_r^t & \cos\theta_p^t \cos\theta_r^t \end{pmatrix} \cdot \begin{pmatrix} 0 \\ 0 \\ dH \end{pmatrix} \\ &= \begin{pmatrix} \cos\theta_p^t \sin\theta_r^t dH \\ -\sin\theta_p^t dH \\ \cos\theta_p^t \cos\theta_r^t dH \end{pmatrix}. \end{aligned} \quad (11)$$

As shown in Figure 2, the integration result of the sensor output is essentially the track along  $dX$  (the black arrows), which can be obtained by Equation (11):

$$dX = dT_L(3) = \cos\theta_p^t \cos\theta_r^t dH. \quad (12)$$

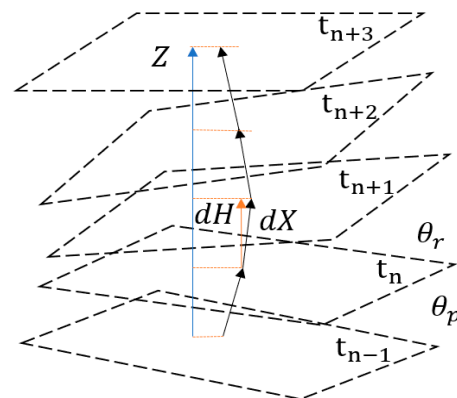


**Figure 2.** Schematic diagram of the acceleration data integration for displacement estimation in tilted conditions.

Based on the relationship of  $dX$  and  $dH$  in Equation (12), the displacement correction function is thus established as

$$Z = \int dH = \int \cos^{-1}\theta_p^t \cos^{-1}\theta_r^t dX, \quad (13)$$

where  $Z$  is the actual displacement of the sensor in the heave direction (the blue arrow).

### 3. Proposed Algorithm

In this work, a multi-sensor fusion ship-borne sensing platform consisting of one gyroscope for angle detection and four piezoelectric acceleration sensors for displacement detection is developed. The proposed sensing system aims to optimize the real-time estimation of the three degrees of freedom of ship-borne mechanical platform movement through two novel multi-sensor fusion algorithms, which will be discussed in detail in the following. The sensor configurations are demonstrated in Figure 3. Four uniaxial acceleration sensors  $S_A$ ,  $S_B$ ,  $S_C$ , and  $S_D$  are installed at the corners of the square platform

with sides of length  $L$ . Moreover, a gyroscope for tilt angle detection is fixed at the center of the square platform.

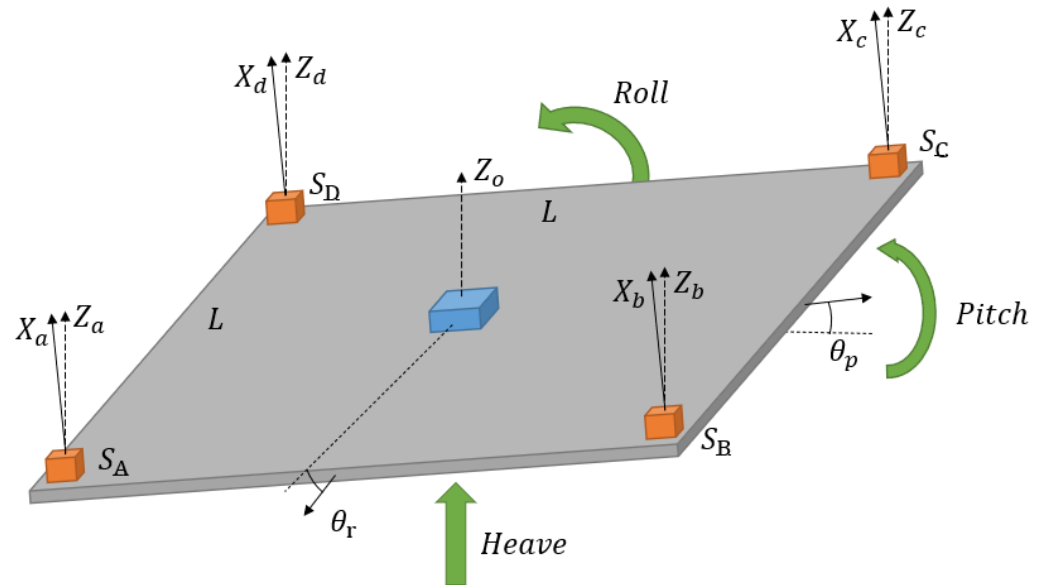


**Figure 3.** Illustration of the proposed multi-sensor fusion ship-borne sensing platform with one gyroscope and four piezoelectric acceleration sensors.

### 3.1. Multi-Sensor Fusion of Acceleration Sensor Sets

In the actual heave direction, four acceleration sensors have displacements of  $Z_a$ ,  $Z_b$ ,  $Z_c$ , and  $Z_d$ , respectively. These displacement values can be obtained by calculating the double integral over time of the sensor outputs. However, due to the unstable tilting motion of the ship-borne mechanical platform, the measured acceleration data tracks the displacement along the direction perpendicular to the mounting base instead. We denote these deflected displacements as  $X_a$ ,  $X_b$ ,  $X_c$ , and  $X_d$ , respectively. As discussed in Section 2, we can theoretically calculate the actual heave displacement according to the available sensor data and the ship-borne mechanical platform motion status as follows:

$$\begin{cases} Z_a(t) = \int_0^t dZ_a + Z_a(0) = \int_0^t \cos^{-1}\theta_p(t) \cos^{-1}\theta_r(t) dX_a + Z_a(0) \\ Z_b(t) = \int_0^t dZ_b + Z_b(0) = \int_0^t \cos^{-1}\theta_p(t) \cos^{-1}\theta_r(t) dX_b + Z_b(0) \\ Z_c(t) = \int_0^t dZ_c + Z_c(0) = \int_0^t \cos^{-1}\theta_p(t) \cos^{-1}\theta_r(t) dX_c + Z_c(0) \\ Z_d(t) = \int_0^t dZ_d + Z_d(0) = \int_0^t \cos^{-1}\theta_p(t) \cos^{-1}\theta_r(t) dX_d + Z_d(0) \end{cases} \quad (14)$$

Considering the real-time operations in the controlling process, the above equation can also be written in discrete forms as follows:

$$\begin{cases} Z_a^t = Z_a^{t-1} + \cos^{-1}\theta_p(t) \cos^{-1}\theta_r(t) V_a^t \Delta t \\ Z_b^t = Z_b^{t-1} + \cos^{-1}\theta_p(t) \cos^{-1}\theta_r(t) V_b^t \Delta t \\ Z_c^t = Z_c^{t-1} + \cos^{-1}\theta_p(t) \cos^{-1}\theta_r(t) V_c^t \Delta t \\ Z_d^t = Z_d^{t-1} + \cos^{-1}\theta_p(t) \cos^{-1}\theta_r(t) V_d^t \Delta t \end{cases} \quad (15)$$

where  $V_a^t$ ,  $V_b^t$ ,  $V_c^t$ , and  $V_d^t$  are the real-time velocities obtained by the four sensor outputs at time  $t$ , respectively.

Because of the known spatial arrangement of the sensor sets, the outputs of four acceleration sensors can be synthetically combined to estimate the tilt angles. The kinematic equation for the pitch angle is as follows:

$$\begin{aligned} \sin\theta_p^t &= \frac{(Z_d^t + Z_c^t) - (Z_a^t + Z_b^t)}{L} \\ &= \frac{1}{L} \left[ \sum_{i=0}^t \cos^{-1}\theta_p^i \cos^{-1}\theta_r^i V_d^i \Delta t + \sum_{i=0}^t \cos^{-1}\theta_p^i \cos^{-1}\theta_r^i V_c^i \Delta t \right. \\ &\quad \left. - \sum_{i=0}^t \cos^{-1}\theta_p^i \cos^{-1}\theta_r^i V_a^i \Delta t - \sum_{i=0}^t \cos^{-1}\theta_p^i \cos^{-1}\theta_r^i V_b^i \Delta t \right] \\ &= \frac{1}{L} \sum_{i=0}^t (-V_a^i - V_b^i + V_c^i + V_d^i) \cos^{-1}\theta_p^i \cos^{-1}\theta_r^i \Delta t. \end{aligned} \quad (16)$$

Similarly, the kinematic equation for the roll angle is

$$\begin{aligned} \sin\theta_r^t &= \frac{(Z_b^t + Z_c^t) - (Z_a^t + Z_d^t)}{L} \\ &= \frac{1}{L} \left[ \sum_{i=0}^t \cos^{-1}\theta_p^i \cos^{-1}\theta_r^i V_b^i \Delta t + \sum_{i=0}^t \cos^{-1}\theta_p^i \cos^{-1}\theta_r^i V_c^i \Delta t \right. \\ &\quad \left. - \sum_{i=0}^t \cos^{-1}\theta_p^i \cos^{-1}\theta_r^i V_a^i \Delta t - \sum_{i=0}^t \cos^{-1}\theta_p^i \cos^{-1}\theta_r^i V_d^i \Delta t \right] \\ &= \frac{1}{L} \sum_{i=0}^t (-V_a^i + V_b^i + V_c^i - V_d^i) \cos^{-1}\theta_p^i \cos^{-1}\theta_r^i \Delta t. \end{aligned} \quad (17)$$

By combining Equations (16) and (17), roll angle and pitch angle can be solved. In this way, an estimation of heave displacement is made in real-time utilizing the above solutions in Equation (15).

### 3.2. Motion Estimation Based on Kalman Filtering

In the previous section, a tilt angle estimation method relying on just four acceleration sensor sets was proposed. Another commonly used ship-borne sensor is the gyroscope for direct angle detection. Generally, piezoelectric acceleration sensors have superior robustness and accuracy due to their direct electromechanical coupling characteristics, whereas angle sensors possess lower drift with the help of gravity. It would greatly improve the precision of motion estimation if these two types of sensor signals were rationally combined. In this work, we adopt the Kalman filtering technique, in which the measurement data from the angle sensor  $\vartheta = [\vartheta_p, \vartheta_r]^T$  is the observation and the computed data from the acceleration sensor sets  $\theta = [\theta_p, \theta_r]^T$  is the estimate. In this case, the system state dynamics in discrete form can be written as

$$\begin{cases} \theta_k = \phi_{k-1}^k \theta_{k-1} + \Gamma_{k-1} W_{k-1}, \\ \vartheta_k = N_k \theta_k + V_k \end{cases}, \quad (18)$$

where  $\theta_k$  and  $\theta_{k-1}$  are the computed angle vectors from acceleration sensor sets at time  $k$  and time  $k-1$ , respectively.  $\phi_{k-1}^k$  denotes the state transition matrix.  $\Gamma_{k-1}$  and  $W_{k-1}$  represent the noise drive matrix and noise vector, respectively.  $\vartheta_k$ ,  $N_k$ , and  $V_k$  are measurement vectors from the angle sensor, measurement matrix, and measurement noise vector at time  $k$ , respectively. Both  $W_{k-1}$  and  $V_k$  are assumed to have zero mean normal distributions with  $E(W_k W_k^T) = 0$  and  $E(V_k V_k^T) = R_k$ , where  $W_k^T$  and  $V_k^T$  are the transposes of vectors  $W_k$  and  $V_k$  respectively, and  $R_k$  is the observation noise covariance matrix.

In the Kalman filtering process, a prior state estimate is first performed using

$$\hat{\theta}_{k-1}^k = \phi_{k-1}^k \hat{\theta}_{k-1}. \quad (19)$$



The prior estimate covariance is

$$P_{k-1}^k = \phi_{k-1}^k P_{k-1} \phi_{k-1}^{kT} + Q_{k-1}. \quad (20)$$

Afterwards, the state estimate is updated based on the observation data and we have the posterior state estimate as

$$\hat{\theta}_k = \hat{\theta}_{k-1}^k + K_k (\vartheta_k - N \hat{\theta}_{k-1}^k), \quad (21)$$

where  $K$  is the optimal Kalman gain, given by

$$K_k = \frac{P_{k-1}^k N_k^T}{N_k P_{k-1}^k N_k^T + R_k}. \quad (22)$$

The posterior estimate covariance is

$$P_k = (I - K_k N_k) P_{k-1}^k. \quad (23)$$

However, it is hard to accurately evaluate the statistical characteristics of noise in both integral error and angle measurement. Such limitations hinder the implementation of Kalman filtering for estimating ship-borne mechanical platform motion in real-time. A robust adaptive filtering technique is thus needed, in which robust estimation theory is applied to eliminate measurement outliers and adaptive factors are incorporated to control the influence of dynamic model error. Given these considerations, we further propose an innovation-based adaptive filtering step to verify the angle measurement results. The procedures are shown as follows: First, the innovation  $\tilde{\vartheta}_{k-1}^k$  and its covariance  $C_k$  are computed by

$$\begin{cases} \tilde{\vartheta}_{k-1}^k = \vartheta_k - N_k \hat{\theta}_{k-1}^k \\ C_k = N_k P_{k-1}^k N_k^T + R_k \end{cases}. \quad (24)$$

Then, we define a weigh boundary value function as

$$\beta = \sqrt{\frac{\vartheta_k^T \vartheta_k}{\text{tr}(C_k)}}, \quad (25)$$

where  $\text{tr}(C_k)$  is the matrix trace of covariance  $C_k$ . The adaptive factor  $\alpha$  is thus determined by

$$\alpha = \begin{cases} 1, & \beta \leq c \\ \frac{c}{\beta}, & \beta > c \end{cases}, \quad (26)$$

where  $c$  is a constant set between 0.9 and 1. Here,  $c = 0.9$  is adopted. We can then adjust the Kalman gain accordingly, as

$$K_k = \frac{1}{\alpha} \cdot \frac{P_{k-1}^k N_k^T}{N_k P_{k-1}^k N_k^T + R_k}. \quad (27)$$

By repeating the two processes of prediction and update, the motion state estimation can be iteratively optimized until the results are converged. The whole Kalman filtering process is schematically illustrated in Figure 4.

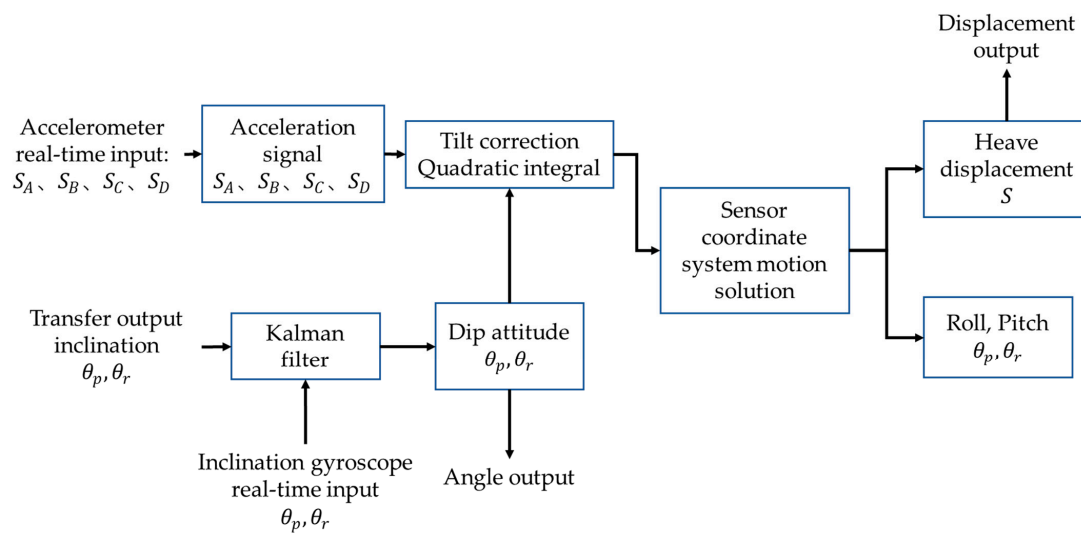


**Figure 4.** Procedure of the proposed Kalman filtering-based motion estimation algorithm by combining acceleration sensor data and angle sensor data.

#### 4. Experimental Results

To experimentally verify the feasibility of the proposed algorithm, we set up the ship-borne mechanical platform with one gyroscope and four piezoelectric acceleration sensors in the lab. As shown in Figure 5, four acceleration sensors were fixed at the corners of a square on the six-degree-of-freedom wave compensation platform (orange points). One gyroscope for angle measurement was placed at the center of the upper plane (blue point). A laser-ranging sensor is installed on the center bracket under the platform (black) to provide the standard heave motion signal for the ship-borne mechanical platform.

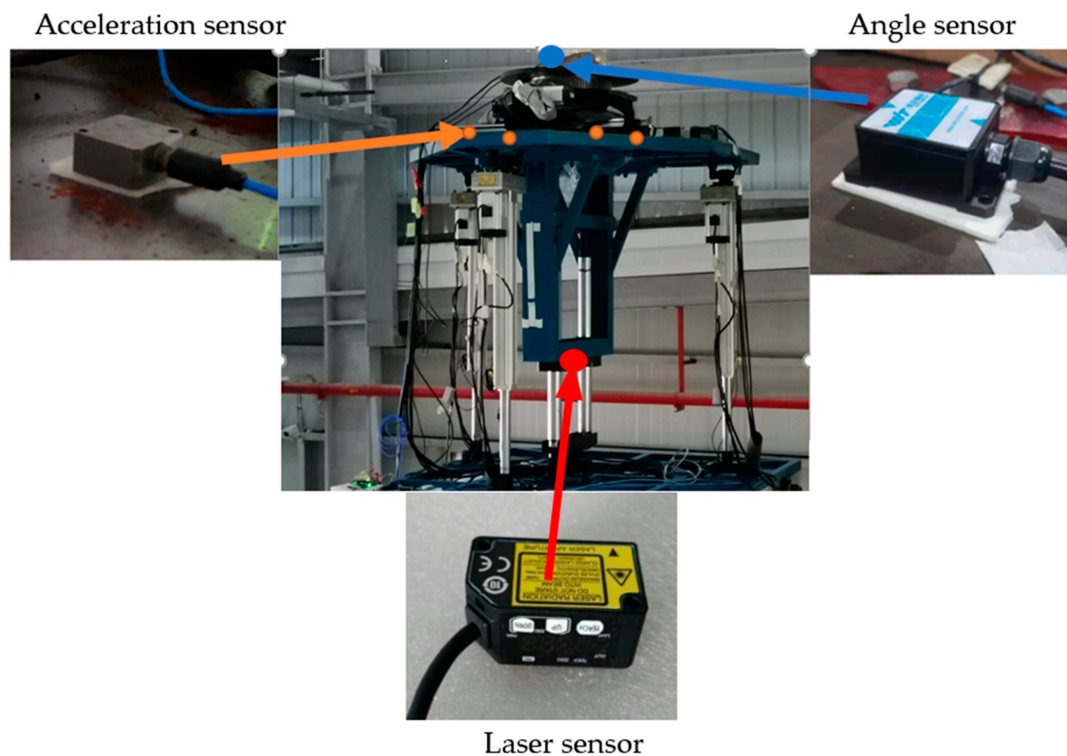


**Figure 5.** Experimental setup for the proposed sensor platform.

In this experiment, we use the WitMotion HWT901B RS232 Sensor. It has the following advantages:

(1) High Precision Pitch Roll (X and Y-axis) Accelerometer + Angular Velocity + Angle + Magnet Field + Air Pressure + Altitude data output. Robust MEMS designs and high performance in harsh environments.

(2) Designed with advanced Kalman filters and a 32-bits processor, it ensures high stability and precision of 0.1–200 Hz data output and a dynamic angle measurement accuracy of 0.05 degree.

(3) In-built with a military-grade RM3100 magnet field sensor, which cannot be affected by magnetic field interference, it can automatically correct the data output to an accurate value.

(4) With extremely high resolution, acceleration (0.005 g), gyroscope ( $0.61^\circ/\text{s}$ ), and magnet field (16 bits).

(5) High angular accuracy after calibration: X, Y-axis:  $0.05^\circ$  (Static), X, Y-axis:  $0.1^\circ$  (Dynamic).

In addition, the laser sensor we use is the Panasonic HG-C series. As compact as a photoelectric sensor, the CMOS laser sensor allows the display of the actual measured distance as accurately as a displacement sensor. It has the following characteristics:

Accurate and Linearity:  $\pm 0.1\%$  F.S.

Compact and Lightweight: W20 mm  $\times$  H44 mm  $\times$  D25 mm

Precise level detection, Repeatability: 10  $\mu\text{m}$

By sending instructions to the servo controller, the ship-borne mechanical platform was controlled to simulate the three-degree-of-freedom movement of the ship. We used a data collector to acquire all sensor data with a sampling frequency of 200 Hz and a sampling time of 100 s. Figure 6 displays the obtained signal after integrating four acceleration sensors, respectively.

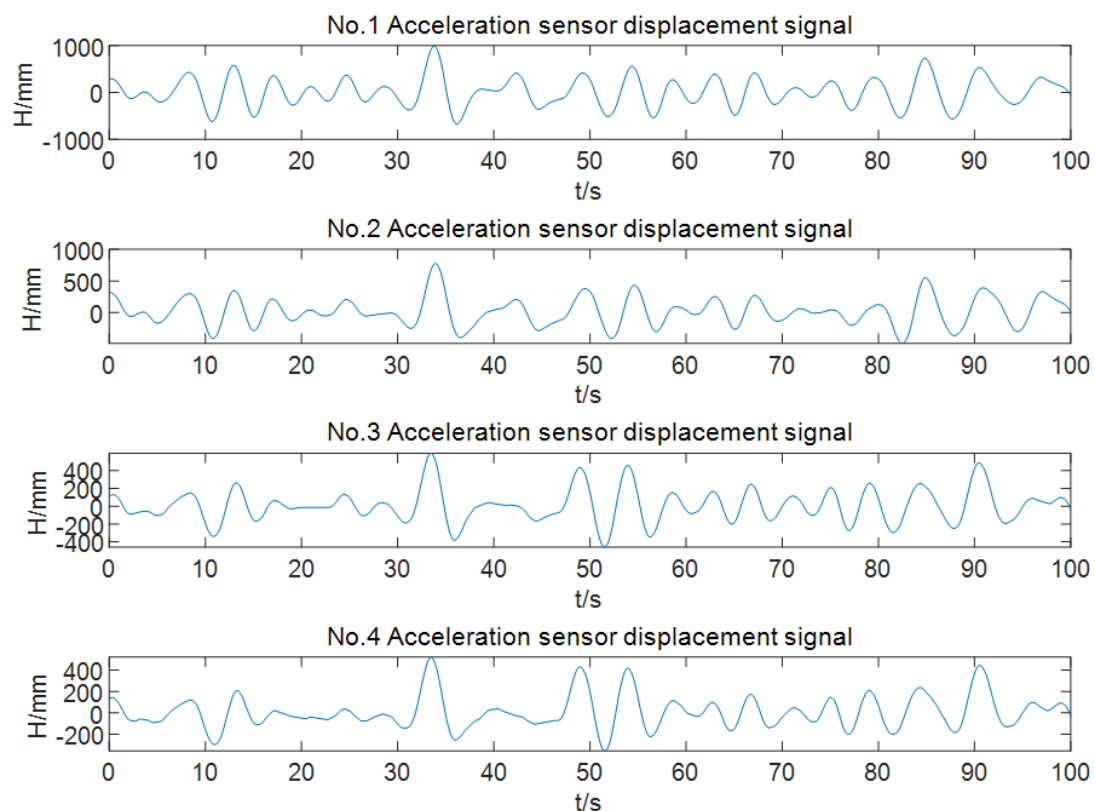


**Figure 6.** Displacement signal obtained by integral of four acceleration sensors outputs.

Pitch and roll angle values for observation input in the filtering process were obtained by the angle sensor. Their outputs are shown in Figure 7.

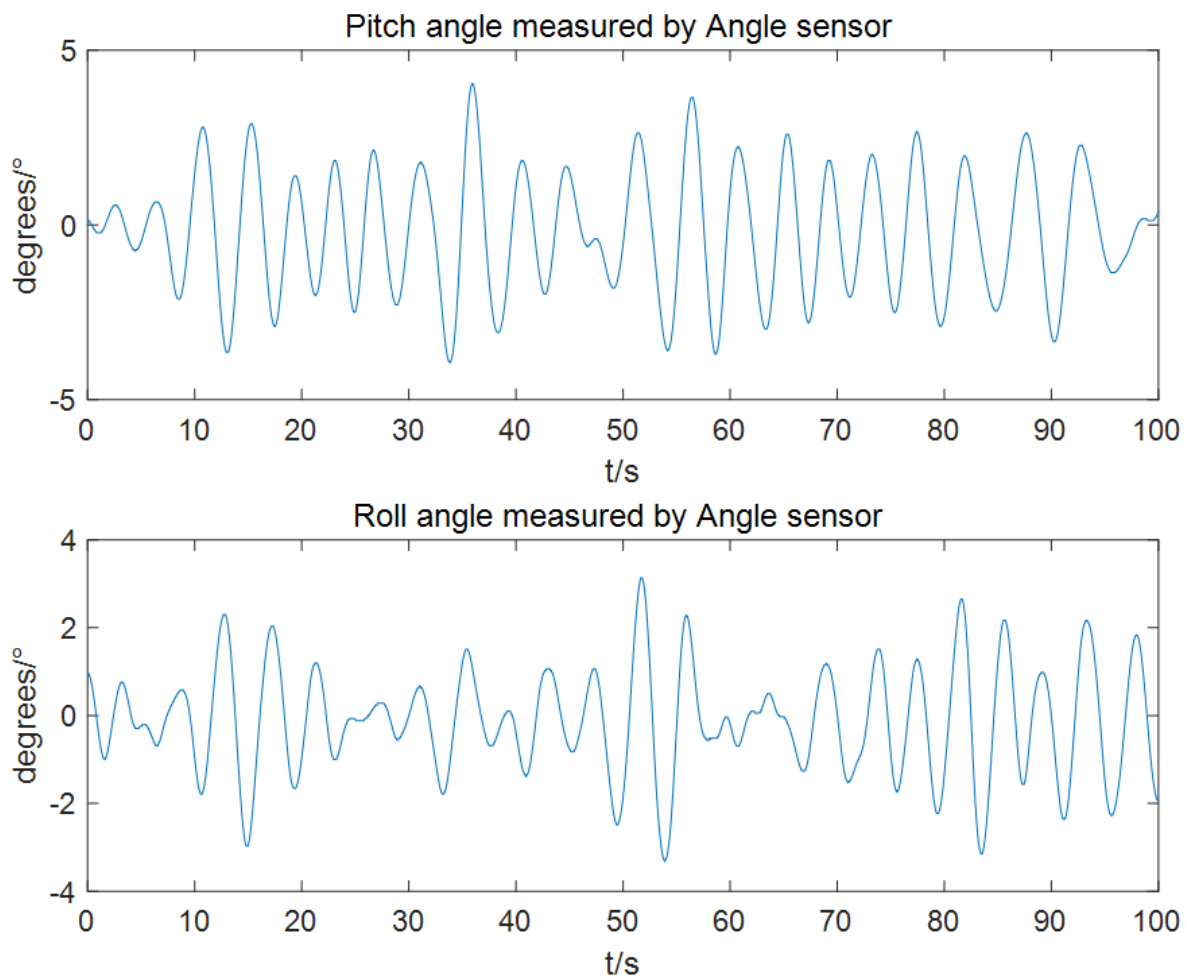


**Figure 7.** Angle signal obtained by angle sensor.

Using the proposed multi-sensor fusion method, the displacement values integrated by the four acceleration sensors were corrected, and the real displacement signal in the heave direction was finally calculated. The estimated displacement signal was compared with the standard displacement signal collected by the laser sensor. The laser displacement signal is considered to be the real heave displacement value of the ship-borne mechanical platform. The data shows that the heave displacement signal corrected based on multi-sensor fusion can effectively improve the accuracy of displacement signal measurement compared with the integrated displacement signal of a single acceleration sensor. The comparison results of the displacement signal based on multi-sensor fusion correction and the displacement signal of the laser sensor are shown in Figure 8. The comparison results of the integrated displacement signal of a single acceleration sensor and the displacement signal of the laser sensor are shown in Figure 9.

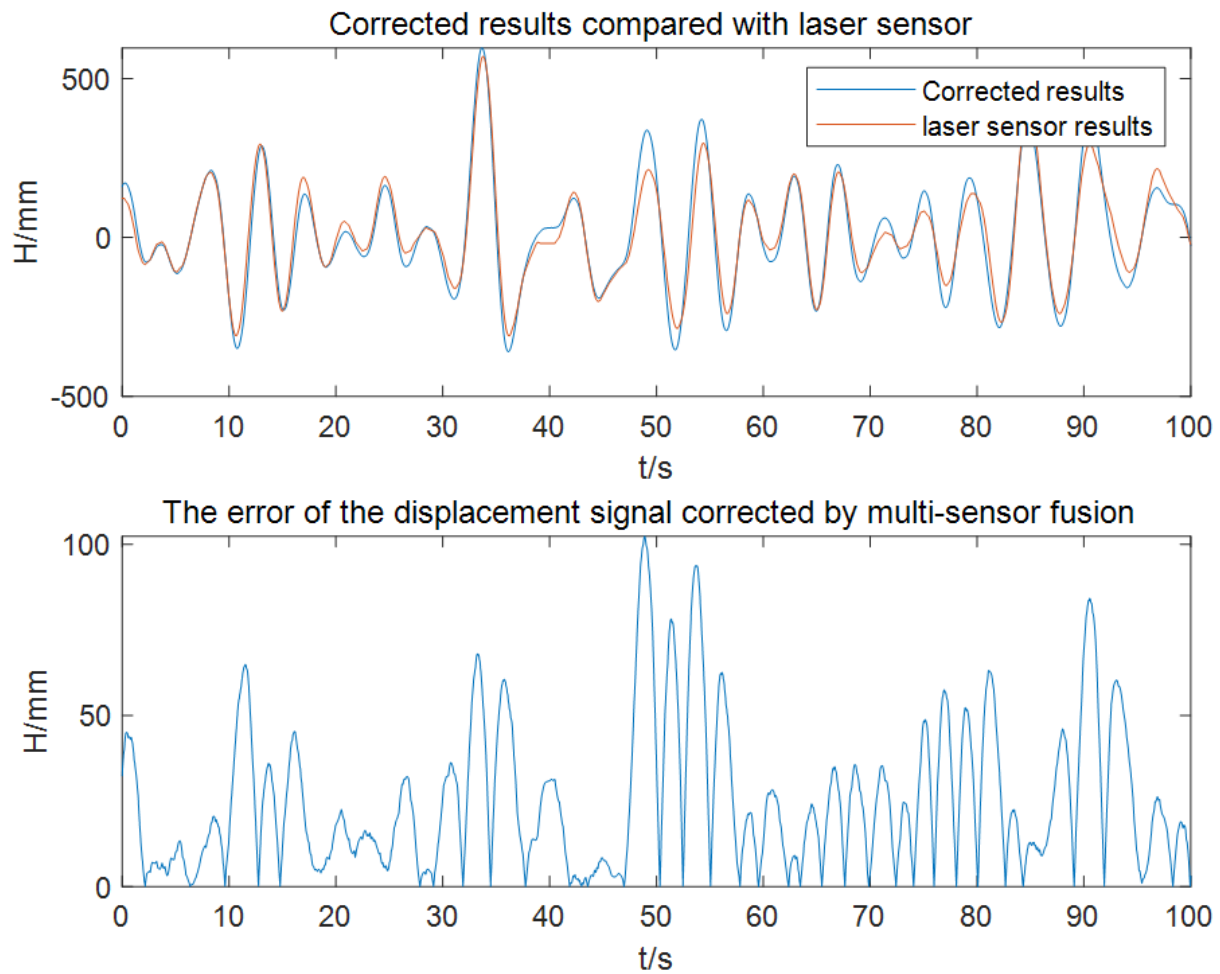


**Figure 8.** The comparison results of the displacement signal based on multi-sensor fusion correction and displacement signal of the laser sensor.

After analyzing the above results, we found that the average error between the displacement signal corrected by using multiple sensors and the laser standard heave displacement signal was 25.34 mm. As a comparison, when a single acceleration sensor was used, the average error of the heave displacement signal denoted by No. 1–4 is [128.1711 mm, 65.32 mm, 73.63 mm, 71.8513 mm].

At the same time, based on multi-sensor fusion data, we used the acceleration sensor to calculate the roll angle signal and pitch angle signal of the ship-borne mechanical platform and performed Kalman filtering on the inclination signal and angle sensor signal to estimate the inclination angle with improved accuracy. Here, the value of our process noise  $Q$  in Kalman filtering was  $[4 \ 0; 0 \ 1]$ ; the value of observation noise variance  $R$  was 1, which made the estimated value more inclined to the angle sensor signal data. The results of the roll angle signal and pitch signal of the ship-borne mechanical platform calculated using the integrated displacement signal of the acceleration sensor are shown in Figure 10. After Kalman filtering with a combination of the angle sensor measurement signal and the calculated angle data through acceleration sensors, the comparison of these three sets of angle information is shown in Figure 11.

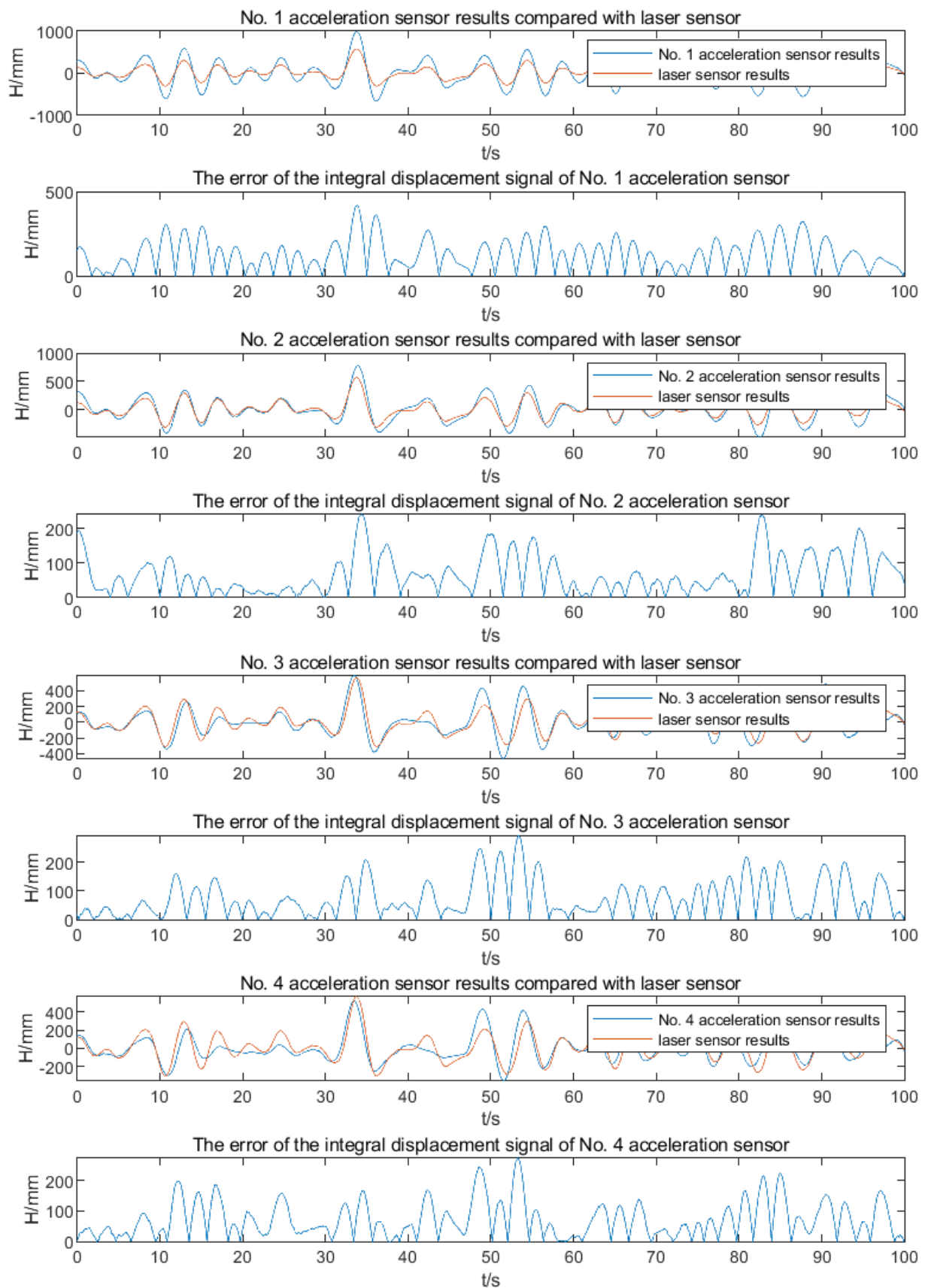


**Figure 9.** The comparison results of the integrated displacement signal of a single acceleration sensor and the displacement signal of the laser sensor.



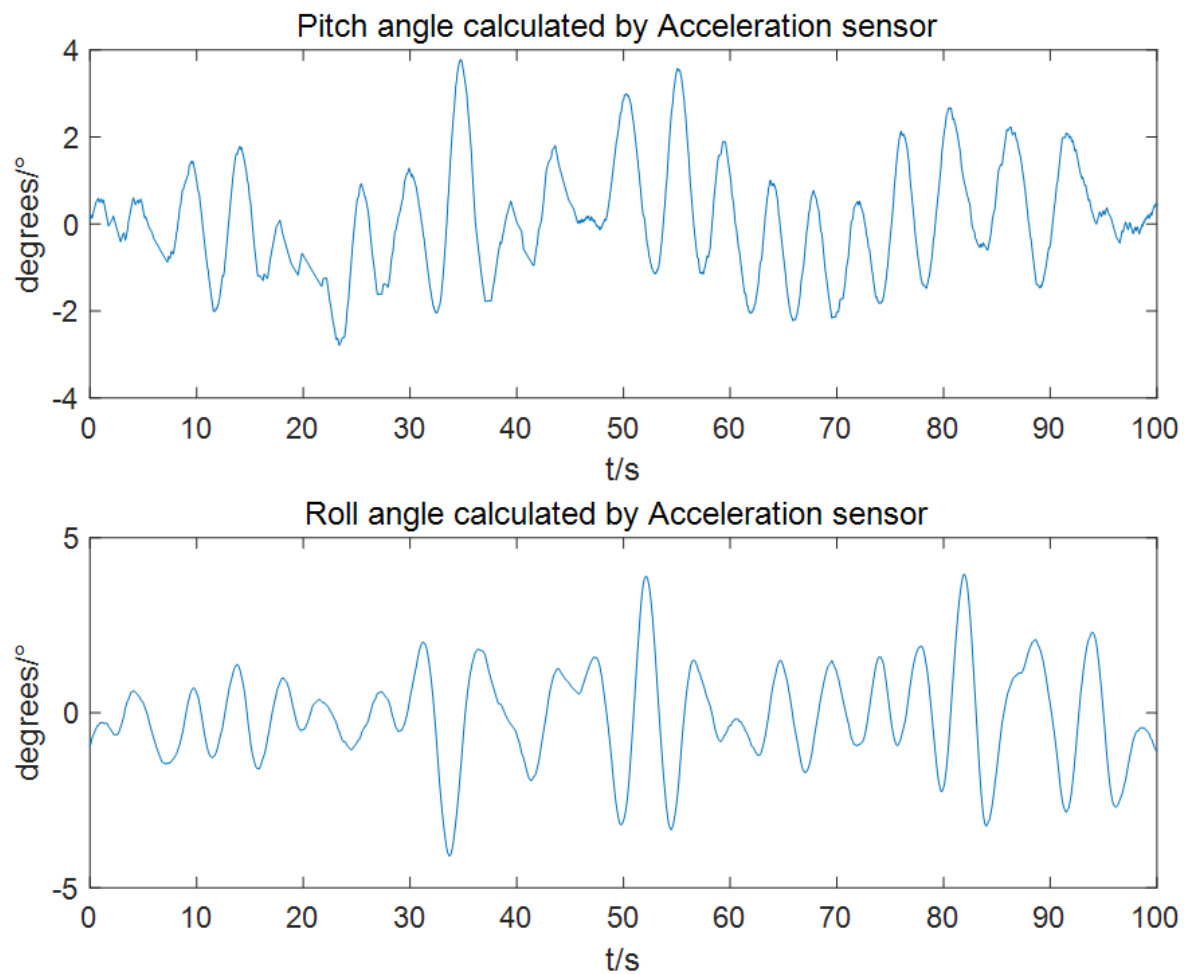


**Figure 10.** The estimated results of the roll angle and pitch angle.

Combining the roll angle and pitch angle signals collected by the angle sensors in Figure 7, correlation analysis was performed on the angle signals calculated based on multiple acceleration sensors. The results showed that the correlation coefficient of the two groups of signals was 0.87, which proved that the inclination signal of the ship-borne mechanical platform calculated by the acceleration sensor was reliable. It can be seen from the experimental results that the angle signal calculated by the acceleration sensor and the angle signal measured by the angle sensor have the following advantages after Kalman filtering:

1. Reduce the influence of noise and error. The angle signal calculated by the acceleration sensor usually has large noise and error. Meanwhile, the angle signal measured by the angle sensor may also be affected by external interference. Through Kalman filtering, these noises and errors can be filtered out so as to obtain more accurate angle signals.
2. Improved response speed. The angle signal calculated by the acceleration sensor has a faster response speed, but there are large noises and errors. On the other hand, the angle signal measured by the angle sensor has a slower response speed but possesses higher precision. Through Kalman filtering, the advantages of the two can be combined, which not only improves the response speed but also improves the accuracy.
3. Improve system stability. Since the angle signal calculated by the acceleration sensor has large noise and errors, the system may jitter or become unstable. Through adaptive Kalman filtering, these noises and errors can be filtered out, thereby improving the stability of the system.

4. Reduced cost: the cost of the angle signal calculated by acceleration sensors is lower than that of the angle signal measured by advanced angle sensors. Through the Kalman filter, the angle signal calculated by the acceleration sensor can be filtered to obtain a result comparable to or even better than the angle signal measured by the angle sensor, thereby reducing the cost of using expensive gyroscopes.

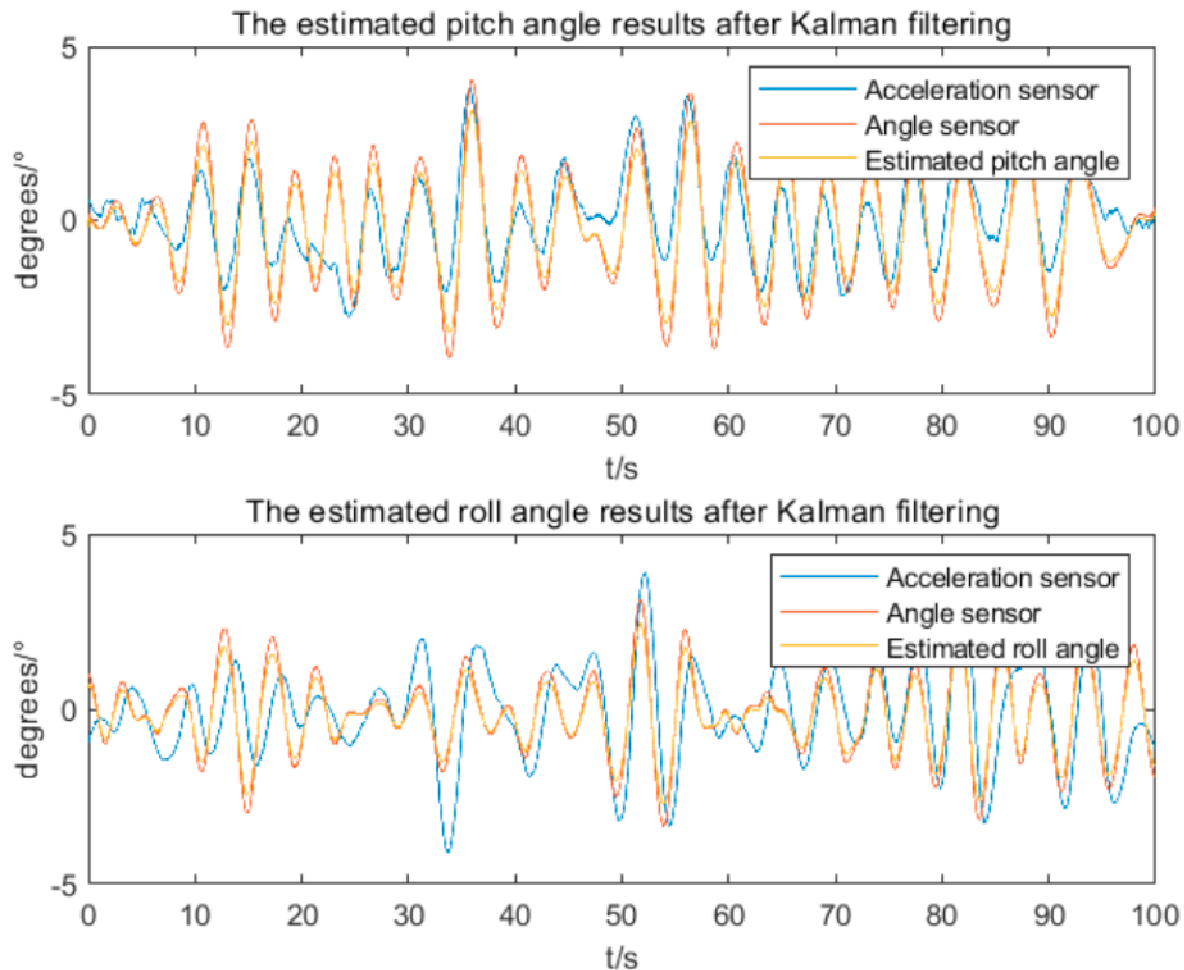


**Figure 11.** Results of estimated pitch and roll angles after Kalman filtering.

## 5. Conclusions

This paper proposes a correction method for shipborne platform motion measurements based on multi-sensor fusion. First, by analyzing the principle of the piezoelectric acceleration sensor, a correction method with a novel configuration of four acceleration sensors is proposed based on the fusion results, which eliminates the influence of the roll angle and pitch angle on the displacement signal after acceleration integration. Secondly, adaptive Kalman filtering is performed to combine the angle signals collected by the angle sensor and the angle signal calculated by the acceleration sensor sets. The estimated inclination angle of the ship-borne mechanical platform showed an improved correlation with the standard motion data obtained by a laser sensor, as verified by the experiments.

The advantage of this method is that it can improve the accuracy of measuring the displacement signal of the ship-borne mechanical platform in the heave direction. It can correct the influence of the roll angle and pitch angle on the integral of the heave direction when the ship-borne mechanical platform moves with three degrees of freedom, eliminate the error caused by the inclination angle, and greatly improve the reliability of the motion signal. At the same time, the disadvantage of this method is that multiple sets of acceleration sensors are used, there is a signal calibration problem, and the sensitivity of



the calibration cannot be well controlled, which will also cause errors in the measurement of the displacement signal.

In the present work, the system we built is based on the fusion of four acceleration sensors to correct the displacement signals of the ship-borne mechanical platform in the heave direction, and by combining the angle sensor data, Kalman filtering is performed on the roll angle signal and the pitch angle signal to estimate the true inclination angle. In future work, we will further study the calibration problem of multiple acceleration sensors. By combining algorithms such as neural networks, the sensors can be calibrated with nonlinear characteristics to overcome the problem of acceleration sensitivity under different sea conditions.

At the same time, in order to reduce costs, we may also look for directions such as the use of inertial mechanical structures for research. By designing a novel inertial mechanical structure instead of multi-sensor fusion to correct the angle effect, the cost of solving the angle effect is further reduced.

**Author Contributions:** Conceptualization, R.Z.; Data curation, X.H.; Formal analysis, R.Z.; Funding acquisition, X.H.; Methodology, R.Z.; Supervision, X.H.; Writing—original draft, R.Z.; Writing—review and editing, R.Z. and X.H. All authors have read and agreed to the published version of the manuscript.

**Funding:** This research was funded by the National Natural Science Foundation of China, grant number 31300783.

**Data Availability Statement:** The original data contributions presented in the study are included in the article; further inquiries can be directed to the corresponding authors.

**Conflicts of Interest:** The authors declare no conflict of interest.

## References

1. Luo, R.C.; Lin, M.-H.; Scherp, R.S. Dynamic Multi-Sensor Data Fusion System for Intelligent Robots. *IEEE J. Robot. Autom.* **1988**, *4*, 386–396. [[CrossRef](#)]
2. Durrant-Whyte, H.F.; Rao, B.Y.S.; Hu, H. Toward a Fully Decentralized Architecture for Multi-Sensor Data Fusion. In Proceedings of the IEEE International Conference on Robotics and Automation, Cincinnati, OH, USA, 13–18 May 1990; IEEE: Piscataway, NJ, USA, 1990; pp. 1331–1336.
3. Wen, W.; Durrant-Whyte, H.F. Model-Based Multi-Sensor Data Fusion. In Proceedings of the 1992 IEEE International Conference on Robotics and Automation, Nice, France, 12–14 May 1992; IEEE: Piscataway, NJ, USA, 1992; pp. 1720–1726.
4. Harris, C.J.; Bailey, A.; Dodd, T.J. Multi-Sensor Data Fusion in Defence and Aerospace. *Aeronaut. J.* **1998**, *102*, 229–244. [[CrossRef](#)]
5. Llinas, J.; Hall, D.L. An Introduction to Multi-Sensor Data Fusion. In Proceedings of the ISCAS'98—1998 IEEE International Symposium on Circuits and Systems (Cat. No. 98CH36187), Monterey, CA, USA, 31 May–3 June 1998; IEEE: Piscataway, NJ, USA, 1998; Volume 6, pp. 537–540.
6. Chen, S.; Bao, H.; Zeng, X.; Yang, Y. A Fire Detecting Method Based on Multi-Sensor Data Fusion. In Proceedings of the SMC'03—2003 IEEE International Conference on Systems, Man and Cybernetics. Conference Theme-System Security and Assurance (Cat. No. 03CH37483), Washington, DC, USA, 8 October 2003; IEEE: Piscataway, NJ, USA, 2003; Volume 4, pp. 3775–3780.
7. Herpel, T.; Lauer, C.; German, R.; Salzberger, J. Multi-Sensor Data Fusion in Automotive Applications. In Proceedings of the 2008 3rd International Conference on Sensing Technology, Taipei, Taiwan, 30 November–3 December 2008; IEEE: Piscataway, NJ, USA, 2008; pp. 206–211.
8. Manjunatha, P.; Verma, A.K.; Srividya, A. Multi-Sensor Data Fusion in Cluster Based Wireless Sensor Networks Using Fuzzy Logic Method. In Proceedings of the 2008 IEEE Region 10 and the Third International Conference on Industrial and Information Systems, Kharagpur, India, 8–10 December 2008; IEEE: Piscataway, NJ, USA, 2008; pp. 1–6.
9. Dong, J.; Zhuang, D.; Huang, Y.; Fu, J. Advances in Multi-Sensor Data Fusion: Algorithms and Applications. *Sensors* **2009**, *9*, 7771–7784. [[CrossRef](#)] [[PubMed](#)]
10. Wolter, P.T.; Townsend, P.A. Multi-Sensor Data Fusion for Estimating Forest Species Composition and Abundance in Northern Minnesota. *Remote Sens. Environ.* **2011**, *115*, 671–691. [[CrossRef](#)]
11. Medjahed, H.; Istrate, D.; Boudy, J.; Baldinger, J.-L.; Dorizzi, B. A Pervasive Multi-Sensor Data Fusion for Smart Home Healthcare Monitoring. In Proceedings of the 2011 IEEE International Conference on Fuzzy Systems (FUZZ-IEEE 2011), Taipei, Taiwan, 27–30 June 2011; IEEE: Piscataway, NJ, USA, 2011; pp. 1466–1473.
12. Banerjee, T.P.; Das, S. Multi-Sensor Data Fusion Using Support Vector Machine for Motor Fault Detection. *Inf. Sci.* **2012**, *217*, 96–107. [[CrossRef](#)]

13. Frikha, A.; Moalla, H. Analytic Hierarchy Process for Multi-Sensor Data Fusion Based on Belief Function Theory. *Eur. J. Oper. Res.* **2015**, *241*, 133–147. [[CrossRef](#)]
14. Azimirad, E.; Haddadnia, J.; Izadipour, A.L.I. A Comprehensive Review of the Multi-Sensor Data Fusion Architectures. *J. Theor. Appl. Inf. Technol.* **2015**, *71*.
15. Fortino, G.; Galzarano, S.; Gravina, R.; Li, W. A Framework for Collaborative Computing and Multi-Sensor Data Fusion in Body Sensor Networks. *Inf. Fusion* **2015**, *22*, 50–70. [[CrossRef](#)]
16. Rawat, S.; Rawat, S. Multi-Sensor Data Fusion by a Hybrid Methodology—A Comparative Study. *Comput. Ind.* **2016**, *75*, 27–34. [[CrossRef](#)]
17. Duro, J.A.; Padget, J.A.; Bowen, C.R.; Kim, H.A.; Nassehi, A. Multi-Sensor Data Fusion Framework for CNC Machining Monitoring. *Mech. Syst. Signal Process.* **2016**, *66*, 505–520. [[CrossRef](#)]
18. Maimaitijiang, M.; Ghulam, A.; Sidike, P.; Hartling, S.; Maimaitiyiming, M.; Peterson, K.; Shavers, E.; Fishman, J.; Peterson, J.; Kadam, S.; et al. Unmanned Aerial System (UAS)-Based Phenotyping of Soybean Using Multi-Sensor Data Fusion and Extreme Learning Machine. *ISPRS J. Photogramm. Remote. Sens.* **2017**, *134*, 43–58. [[CrossRef](#)]
19. Jing, L.; Wang, T.; Zhao, M.; Wang, P. An Adaptive Multi-Sensor Data Fusion Method Based on Deep Convolutional Neural Networks for Fault Diagnosis of Planetary Gearbox. *Sensors* **2017**, *17*, 414. [[CrossRef](#)] [[PubMed](#)]
20. Kumar, P.; Gauba, H.; Roy, P.P.; Dogra, D.P. Coupled HMM-Based Multi-Sensor Data Fusion for Sign Language Recognition. *Pattern Recognit. Lett.* **2017**, *86*, 1–8. [[CrossRef](#)]
21. Bouain, M.; Ali, K.M.A.; Berdjag, D.; Fakhfakh, N.; Atitallah, R. Ben An Embedded Multi-Sensor Data Fusion Design for Vehicle Perception Tasks. *J. Commun.* **2018**, *13*, 8–14. [[CrossRef](#)]
22. Xiao, F.; Qin, B. A Weighted Combination Method for Conflicting Evidence in Multi-Sensor Data Fusion. *Sensors* **2018**, *18*, 1487. [[CrossRef](#)]
23. Zhang, W.; Ning, Y.; Suo, C. A Method Based on Multi-Sensor Data Fusion for UAV Safety Distance Diagnosis. *Electronics* **2019**, *8*, 1467. [[CrossRef](#)]
24. De Farias, C.M.; Pirmez, L.; Fortino, G.; Guerrieri, A. A Multi-Sensor Data Fusion Technique Using Data Correlations among Multiple Applications. *Future Gener. Comput. Syst.* **2019**, *92*, 109–118. [[CrossRef](#)]
25. Xiao, F. Multi-Sensor Data Fusion Based on the Belief Divergence Measure of Evidences and the Belief Entropy. *Inf. Fusion* **2019**, *46*, 23–32. [[CrossRef](#)]
26. Xiao, F. Evidence Combination Based on Prospect Theory for Multi-Sensor Data Fusion. *ISA Trans.* **2020**, *106*, 253–261. [[CrossRef](#)]
27. Muzammal, M.; Talat, R.; Sodhro, A.H.; Pirbhulal, S. A Multi-Sensor Data Fusion Enabled Ensemble Approach for Medical Data from Body Sensor Networks. *Inf. Fusion* **2020**, *53*, 155–164. [[CrossRef](#)]
28. Li, N.; Gebrael, N.; Lei, Y.; Fang, X.; Cai, X.; Yan, T. Remaining Useful Life Prediction Based on a Multi-Sensor Data Fusion Model. *Reliab. Eng. Syst. Saf.* **2021**, *208*, 107249. [[CrossRef](#)]
29. Kashinath, S.A.; Mostafa, S.A.; Mustapha, A.; Mahdin, H.; Lim, D.; Mahmoud, M.A.; Mohammed, M.A.; Al-Rimy, B.A.S.; Fudzee, M.F.M.; Yang, T.J. Review of Data Fusion Methods for Real-Time and Multi-Sensor Traffic Flow Analysis. *IEEE Access* **2021**, *9*, 51258–51276. [[CrossRef](#)]
30. Fei, S.; Hassan, M.A.; Xiao, Y.; Su, X.; Chen, Z.; Cheng, Q.; Duan, F.; Chen, R.; Ma, Y. UAV-Based Multi-Sensor Data Fusion and Machine Learning Algorithm for Yield Prediction in Wheat. *Precis. Agric.* **2023**, *24*, 187–212. [[CrossRef](#)] [[PubMed](#)]
31. Han, C.; Hu, X. An Absolute Displacement Measurement Method and Its Application in Ship Motion Measurement. *J. Mar. Sci. Eng.* **2023**, *11*, 931. [[CrossRef](#)]
32. Wright, R.G. Intelligent Autonomous Ship Navigation Using Multi-Sensor Modalities. *TransNav Int. J. Mar. Navig. Saf. Sea Transp.* **2019**, *13*, 503–510. [[CrossRef](#)]
33. Ma, R.; Yin, Y.; Li, Z.; Chen, J.; Bao, K. Research on Active Intelligent Perception Technology of Vessel Situation Based on Multisensor Fusion. *Math. Probl. Eng.* **2020**, *2020*, 9146727. [[CrossRef](#)]
34. Ali, U.; Muhammad, W.; Irshad, M.J.; Manzoor, S. Multi-Sensor Fusion for Underwater Robot Self-Localization Using PC/BC-DIM Neural Network. *Sens. Rev.* **2021**, *41*, 449–457. [[CrossRef](#)]
35. Higgins, E.; Sobien, D.; Freeman, L.; Pitt, J.S. Ship Wake Detection Using Data Fusion in Multi-Sensor Remote Sensing Applications. In Proceedings of the AIAA SCITECH 2022 Forum, San Diego, CA, USA, 3–7 January 2022; p. 0997.

**Disclaimer/Publisher's Note:** The statements, opinions and data contained in all publications are solely those of the individual author(s) and contributor(s) and not of MDPI and/or the editor(s). MDPI and/or the editor(s) disclaim responsibility for any injury to people or property resulting from any ideas, methods, instructions or products referred to in the content.